Entanglement production in a quantum heat engine

Author
Elias Nyholm

Supervisor
Peter Samuelsson
Co-supervisor
Patrick Potts

Thesis submitted for the degree of Bachelor of Science
Project duration: 2 months

LUND UNIVERSITY

Department of Physics | Division of Mathematical Physics | May 2020

Abstract

Entanglement production is one of the properties of interest when studying nanoscale systems. Not only does entanglement between subsystems hints at other non-classical behaviour and effects that may be of interest to applications; the resource of entangled systems themselves is one on which many future devices and protocols may depend on [1]. In this thesis work, a system of two quantum dots coupled in series between two fermionic leads is considered. The system is a fermionic version of the qubit system studied previously by J. B. Brask et. al. [2]. Assuming steady state, the density matrix of the double dot subsystem is calculated by first finding the retarded Green's functions of the system, and then showing the connection between these Green's functions and the elements of the density matrix. From the density matrix, the entanglement produced between the two quantum dots is extracted. This result is compared to and shown to agree with previous theoretical results, where instead a Markovian master equation approach was used to find the density matrix. Finally, in the discussion and outlook sections possible next steps in the calculation are discussed, as well as the advantages of the Green's functions method over the Markovian master equation approach.

Acknowledgements

I would like to thank my supervisors Peter Samuelsson and Patrick Potts for providing me with such an interesting bachelor work. I have learned a lot, and all the help and feedback during this period has been invaluable.

I would also like to thank Lucas Knuthson, Love Petterson and Ashar Kamal for interesting discussions during the period, and for reading through and giving feedback on this report.

Contents

1 Introduction

The study of nanoscale devices and systems has grown substantially over the recent decades, with research communities thriving on both the theoretical [3,4] and experimental [5,6] sides. Nanostructures such as quantum dots and nanowires can now be created experimentally in laboratories [7, 8], which allows for the creation of systems simple enough to be modelled accurately by pen-and-paper calculations. The applications of such nanostructures range from heat engines [9] and clocks [10] based on thermodynamical properties, to quantum entanglers [2, 11] and beyond. The efficient production of entangled states has been studied extensively [12, 13], as the resource of entangled states is vital for applications in the fields of quantum computing and quantum cryptography among others [1].

These nanosystems, like many other systems studied in contemporary physics, require a quantum-mechanical treatment to be modelled accurately. Open quantum systems, i.e. quantum systems which interact with some environment, are represented mathematically by the density matrix. The density matrix generalizes the notion of a state ket from quantum mechanics, and is used to extract thermodynamical and entanglement properties. Therefore, solving such a system often refers to calculating the density matrix. This quantity is commonly calculated by the use of Markovian master equations [14]. The Markovian master equation method is generally based on strong approximations, but where these approximations are accurate they can be used to calculate the density matrix.

This thesis work will focus on a particular system of two quantum dots coupled in series between two fermionic leads. This is a fermionic version of a qubit system previously studied by the use of Markovian master equations [2, 11, 15]. Instead of the Markovian master equation method we will make use of Green's functions to calculate the density matrix and extract the concurrence of the quantum dot subsystem. Unlike the solutions to Markovian master equations, Green's functions are exact solutions to the problem at hand. The system will be modeled without interaction; introducing interaction such as Coloumb repulsion and attraction would generally require a perturbative solution of the Green's functions.

2 Theory

Throughout this thesis, we set $\hbar = 1$. The equations in each of the subsections can be found in the references of that particular subsection.

2.1 Heisenberg and Schrödinger picture

The dynamics of quantum mechanics are commonly formulated in one of three formalisms. Only two of these, the Heisenberg and Schrödinger pictures, are relevant to this thesis. The third one is the interaction picture, which will not be covered further here. In the Schrödinger picture state kets are time-dependent, $|\psi\rangle = |\psi(t)\rangle$. The dynamics of the states in a system with Hamiltonian $\hat{H}$ are governed by the Schrödinger equation [16]

$$i\frac{\mathrm{d}\,|\psi(t)\rangle}{\mathrm{d}t} = \hat{H}\,|\psi(t)\rangle\,. \tag{1}$$

In the case of a time-independent Hamiltonian, the Schrödinger equation is equivalent to the explicit time evolution of state kets

$$|\psi(t_2)\rangle = \hat{\mathcal{U}}(t_2, t_1)\,|\psi(t_1)\rangle\,, \qquad \hat{\mathcal{U}} \equiv \exp\left[-i\hat{H}(t_2 - t_1)\right]. \tag{2}$$

In this picture, operators corresponding to observables such as $\hat{x}$ and $\hat{p}$ are stationary in time; any change in measurement probabilities over time is due to the state ket $|\psi(t)\rangle$ changing.

In the Heisenberg picture however, state kets are independent of time. Instead, operators evolve in time according to the Heisenberg equation of motion

$$i\frac{\mathrm{d}\hat{A}(t)}{\mathrm{d}t} = [\hat{A}, \hat{H}]. \tag{3}$$

Here it is assumed that $\hat{A}$ has no explicit time dependence in the Schrödinger picture, which would otherwise introduce one additional term in (3). For a time-independent Hamiltonian, the solution to the Heisenberg equation of motion is

$$\hat{A}(t_2) = \hat{\mathcal{U}}(t_2, t_1)\hat{A}(t_1)\hat{\mathcal{U}}^{\dagger}(t_2, t_1) = \hat{\mathcal{U}}(t_2, t_1)\hat{A}(t_1)\hat{\mathcal{U}}(t_1, t_2). \tag{4}$$

The two pictures are completely equivalent. They should however not be mixed, as operators and states are equal only between the pictures at some pre-specified overlapping point in time.

All equations in this subsection are taken from [16].

2.2 The second quantization formalism

Many-particle quantum physics is commonly formulated in the second quantization formalism [17], where the entire system is described by kets indexed by occupation numbers. Any single such ket

$$|n_1, n_2, n_3, \ldots\rangle \tag{5}$$

is an eigenket to the occupation number operators $\hat{n}_i$. The eigenvalue of a specific number operator $\hat{n}_k$ is the number of particles occupying the state indexed by k

$$\hat{n}_k \, |n_1, n_2, \ldots, n_k, \ldots\rangle = n_k \, |n_1, n_2, \ldots, n_k, \ldots\rangle \, . \tag{6}$$

The focus in this thesis is on fermionic systems, where the occupation numbers can equal either 0 or 1. The formalism can also be developed in a similar fashion for bosonic systems and is covered in most introductory literature on many-body physics, e.g. [17]. The occupation number operator can be factorized into one creation and one annihilation operator, $\hat{c}^\dagger$ and $\hat{c}$ respectively, where one is the hermitian conjugate of the other

$$\hat{n}_k = \hat{c}_k^\dagger \hat{c}_k. \tag{7}$$

The creation and annihilation operators add and subtract one particle from one state in the system. However if this would put the occupation number outside the allowed range $\{0, 1\}$, the ket is mapped to zero

$$\hat{c}_k^\dagger \, |\ldots, n_k, \ldots\rangle = \begin{cases} |\ldots, n_k + 1, \ldots\rangle \, , & n_k = 0 \\ 0, & n_k = 1 \end{cases} \tag{8}$$

$$\hat{c}_k \, |\ldots, n_k, \ldots\rangle = \begin{cases} 0, & n_k = 0 \\ |\ldots, n_k - 1, \ldots\rangle \, , & n_k = 1. \end{cases} \tag{9}$$

This allows all second quantization kets (5) to be expressed as creation operators operating on the empty (vacuum) state $|0, 0, 0, \ldots\rangle$

$$|n_1, n_2, n_3, \ldots\rangle = (\hat{c}_1^\dagger)^{n_1} (\hat{c}_2^\dagger)^{n_2} (\hat{c}_3^\dagger)^{n_3} \cdots |0, 0, 0, \ldots\rangle \, . \tag{10}$$

The majority of calculations carried out in the second quantization formalism is not on the kets themselves, but on the creation and annihilation operators. Central properties of

these operators include the anti-commutator relations

$$\{\hat{c}_j^\dagger, \hat{c}_k^\dagger\} = 0, \quad \{\hat{c}_j, \hat{c}_k\} = 0, \quad \{\hat{c}_j, \hat{c}_k^\dagger\} = \delta_{jk}. \tag{11}$$

Note that in general these operators do not commute $[\hat{c}_j^\dagger, \hat{c}_k^\dagger] \neq 0$, which means that the ordering of annihilation and creation operators, such as in (10), is of significance.

All equations in this subsection are taken from [17].

2.3 The density matrix

The density matrix is a generalization of the state ket, and is commonly used to describe statistical ensembles of states [18]. States which can be described by a state ket are pure states, while any state that is not pure is called mixed. A density matrix describing a system in a statistical ensemble of pure states $\{|\psi_i\rangle\}$ is defined as

$$\hat{\rho} = \sum_i p_i \, |\psi_i\rangle \, \langle\psi_i| \tag{12}$$

where the set of real constants $\{p_i\}$ are the statistical weights of the ensemble [19]. The interpretation of $\{p_i\}$ as probabilities justifies the conditions $0 < p_i \leq 1$, $\sum_i p_i = 1$ which we impose on the weights.

Since in the most general case, the density matrix is our description of the system at hand, there should be a way to define the expectation value $\langle\hat{A}\rangle$ of an operator $\hat{A}$ in a system described by $\hat{\rho}$. This expectation value is defined as

$$\langle\hat{A}\rangle = \mathrm{Tr}\{\hat{\rho}\hat{A}\} \tag{13}$$

which is a direct generalization of the familiar expression for pure states $\langle\hat{A}\rangle = \langle\psi|\hat{A}|\psi\rangle$. Here $\mathrm{Tr}\{\hat{A}\}$ denotes the trace

$$\mathrm{Tr}\{\hat{A}\} = \sum_i \langle\phi_i|\hat{A}|\phi_i\rangle \tag{14}$$

which is independent of the choice of complete orthonormal basis $\{|\phi_i\rangle\}$.

Eqs. (12) and (14) are taken from [19]. Eq. (13) is taken from [17].

2.4 Green's functions

In mathematics, Green's functions $G_{ij}(t,t')$ are inverse functions to some linear operator $\mathcal{L}$. That is, the linear operator maps Green's functions to Dirac delta functions

$$\mathcal{L}[G_{ij}(t,t')] = \delta_{ij}\delta(t-t'). \tag{15}$$

The Dirac delta function is a generalized function which can be defined from its Fourier transform as

$$\delta(t-t') = \frac{1}{2\pi}\int_{-\infty}^{\infty} e^{-i\omega(t-t')}d\omega = \begin{cases} 0, & t \neq t' \\ \infty, & t = t' \end{cases} \tag{16}$$

and the Kronecker delta is defined as

$$\delta_{ij} = \begin{cases} 0, & i \neq j \\ 1, & i = j. \end{cases} \tag{17}$$

The discrete indexing i, j can be replaced with one or several pairs of continuous variables x, x', see for example [20]. Green's functions are frequently used to solve linear differential equations on the form

$$\mathcal{L}[f_i(t)] = g_i(t) \tag{18}$$

since if the Green's function of $\mathcal{L}$ is known, the solution to (18) is given by

$$f_i(t) = \sum_j \int G_{ij}(t,t')g_j(t')dt'. \tag{19}$$

This can be seen by explicit calculation since the operator only acts on the non-primed variables

$$\mathcal{L}[f_i(t)] = \mathcal{L}\left[\sum_j \int G_{ij}(t,t')g_j(t')dt'\right] \tag{20}$$

$$= \sum_j \int \mathcal{L}\left[G_{ij}(t,t')\right] g_j(t')dt' \tag{21}$$

$$= \sum_j \delta_{ij} \int \delta(t-t')g_j(t')dt' \tag{22}$$

$$= g_i(t). \tag{23}$$

In physics, Green's functions are used to encode the past and future evolution of a par-

ticle/state [21]. They provide a method to solving a physical system exactly, in terms of its behaviour, properties and dynamics. In quantum mechanics, the relevant differential operator is the Schrödinger operator

$$\mathcal{L} = i\frac{\mathrm{d}}{\mathrm{d}t} - H_{ij} \tag{24}$$

where H_{ij} are elements of the Hamiltonian in a discrete basis.

The defining equation (24) of the Green's function has a range of solutions. A boundary condition is imposed to end up with the Green's function of choice. The solution with boundary condition $t < t' \implies G_{ij}(t,t') = 0$ is called the retarded Green's function [17] and is given by

$$G^{+}_{ij}(t,t') = -i\theta(t-t')\langle\left\{\hat{c}_i(t), \hat{c}^{\dagger}_j(t')\right\}\rangle. \tag{25}$$

Here $\theta(t)$ is the Heaviside step function defined as

$$\theta(t) = \begin{cases} 1, & \text{if } t > 0 \\ 0, & \text{otherwise.} \end{cases} \tag{26}$$

The time-dependence of the second quantization operators are governed by the Heisenberg equation (3). The boundary condition $t > t' \implies G_{ij}(t,t') = 0$ yields the advanced Green's function

$$G^{-}_{ij}(t,t') = i\theta(t'-t)\langle\left\{\hat{c}_i(t), \hat{c}^{\dagger}_j(t')\right\}\rangle. \tag{27}$$

A third kind are the lesser Green's functions, which are not solutions to (24) but closely related to (25) and (27):

$$G^{<}_{ij}(t,t') = i\langle\hat{c}^{\dagger}_j(t')\hat{c}_i(t)\rangle. \tag{28}$$

If the Hamiltonian of the system is time-independent then the Green's functions only depend on the time difference $t-t'$. It is then convenient to do calculations in frequency space where the Green's functions depend only on a single variable

$$G_{ij}(\omega) = \mathcal{F}[G_{ij}(t-t')] = \int_{-\infty}^{\infty} dt G_{ij}(t-t')e^{i\omega(t-t')}. \tag{29}$$

One useful relation in the frequency domain is that the retarded and advanced Green's functions are closely related

$$G^{-}_{ij}(\omega) = \left[G^{+}_{ji}(\omega)\right]^{*}. \tag{30}$$

Eqs. (15) to (20) are taken from [20]. Eqs. (24) to (30) are taken from [17].

2.5 Entanglement

If two separate, uncoupled quantum systems are considered, the state of the total system is given by a product state. A product state is a state of the full system AB that can be written as a tensor product of a state ket in subsystem A and a state ket in subsystem B

$$|\Psi\rangle_{AB} = |\psi\rangle_A \otimes |\phi\rangle_B . \tag{31}$$

In this case, the two states $|\psi\rangle_A$ and $|\phi\rangle_B$ are completely independent of each other; interacting with one of the subsystems will not change the state of the other one. If interaction between the subsystems is introduced, or if the full system AB is interacted with, the most general state of the composite system is a linear combination of product states

$$|\Phi\rangle_{AB} = \sum_i c_i |\psi_i\rangle_A \otimes |\phi_i\rangle_B . \tag{32}$$

If the composite state $|\Phi\rangle_{AB}$ can not be reduced to a product on the form (31), it is called an entangled state [1]. More generally, if the state of the composite system is described by some density matrix ρ^{AB}, the state of the system is called a product state if it can be written on the form

$$\rho^{AB} = \sum_i \omega_i \rho_i^A \otimes \rho_i^B. \tag{33}$$

States described by density matrices that are not product states are called entangled states.

2.5.1 Concurrence

To quantify the entanglement in a two-qubit system, concurrence is commonly used. Define the bit-flipped density matrix as

$$\tilde{\rho} = (\sigma_y \otimes \sigma_y)\hat{\rho}^*(\sigma_y \otimes \sigma_y) \tag{34}$$

where σ_y is the Pauli y-matrix. Also, denote by $\lambda_1, \lambda_2, \lambda_3, \lambda_4$ the eigenvalues of the matrix $R = \hat{\rho}\tilde{\rho}$, ordered in decreasing magnitude. Then the concurrence of the system described by $\hat{\rho}$ is defined as

$$\mathcal{C}\{\hat{\rho}\} = \max\{0, \sqrt{\lambda_1} - \sqrt{\lambda_2} - \sqrt{\lambda_3} - \sqrt{\lambda_4}\}. \tag{35}$$

This is well-defined since $\hat{\rho}$ is positive semi-definite, which implies that all the eigenvalues of R are non-negative.

All equations in this subsection are taken from [1].

3 The system

The system considered in this thesis is a fermionic version of the qubit system studied by J. B. Brask et al. [2]. The system consists of two quantum dots coupled in series between two thermal baths, see Fig. 1. Throughout this thesis, the complete system will be denoted by $\mathcal{S}$, the leads sub-system will be denoted by $\mathcal{S}_l$ and the sub-system consisting of only the two quantum dots by $\mathcal{S}_D$. The same subscripts will also be used for matrices.

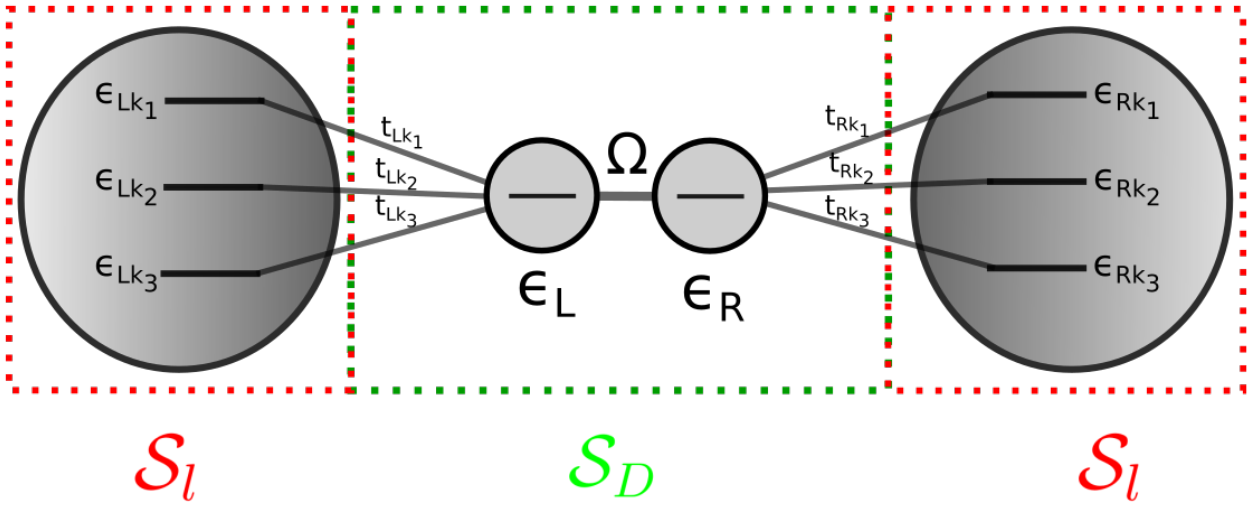

Figure 1: Illustration of the physical system treated in this thesis. S_l and S_D denotes the subsystems consisting of only the heat baths and the quantum dots, respectively. ϵ denotes the energy level of a site in the system, Ω denotes the inter-dot coupling and t denotes the coupling strength between a quantum dot and its respective heat bath.

3.1 Hamiltonian and mathematical properties

The Hamiltonian of the system is given by

$$\hat{H} = \hat{H}_0 + \hat{V} \tag{36}$$

where the uncoupled part is

$$\hat{H}_0 = \sum_{\alpha} \epsilon_\alpha \hat{d}_\alpha^\dagger \hat{d}_\alpha + \sum_{\alpha} \sum_{k} \epsilon_{\alpha k} \hat{c}_{\alpha k}^\dagger \hat{c}_{\alpha k}. \tag{37}$$

Here $\alpha \in \{\mathrm{L}, \mathrm{R}\}$ and k runs over all the energy levels in the respective thermal bath. To follow conventions, $\hat{d}$ is used instead of $\hat{c}$ to denote the second quantization operators in $\mathcal{S}_D$. The interaction term $\hat{V}$ is given by

$$\hat{V} = \Omega(\hat{d}_{\mathrm{L}}^{\dagger}\hat{d}_{\mathrm{R}} + \hat{d}_{\mathrm{R}}^{\dagger}\hat{d}_{\mathrm{L}}) + \sum_{\alpha}\sum_{k}\left(t_{\alpha k}\hat{c}_{\alpha k}^{\dagger}\hat{d}_{\alpha} + t_{\alpha k}^{*}\hat{d}_{\alpha}^{\dagger}\hat{c}_{\alpha k}\right) \tag{38}$$

where the constant Ω characterises the coupling strength between the two quantum dots, while the constants $t_{\alpha k}$ characterises the coupling strength between quantum dot α and thermal bath level αk. Coulomb interaction between electrons is not taken into consideration in this model. The interaction would introduce terms with four fermionic operators into the Hamiltonian, such as $\hat{c}_L^{\dagger}\hat{c}_R^{\dagger}\hat{c}_R\hat{c}_L$, which would make calculating the Green's function much more challenging.

4 Calculations

In Section 4.1, the retarded Green's functions of the system are calculated. This result is then used in Section 4.2 to calculate the lesser Green's functions. When evaluated at equal times $t = t'$, the lesser Green's functions are directly related to the components of the density matrix. This relation is shown in Section 4.3.

4.1 Retarded Green's functions

The starting point is some simpler Hamiltonian and the Green's function of that system; in this case the Hamiltonian of the uncoupled system (37). To find the retarded Green's functions for the uncoupled system, here denoted as g^{+}, we use the equations of motion method. This involves evaluating the time derivative of the Green's functions. Evaluating the time derivative of the (so far unknown) uncoupled Green's functions

$$\begin{aligned} i\partial_t g^{+}_{\gamma\gamma'}(t,t') &= \partial_t\theta(t-t')\langle\left\{\hat{c}_\gamma(t), \hat{c}^{\dagger}_{\gamma'}(t')\right\}\rangle - i\theta(t-t')\langle\left\{i\partial_t\hat{c}_\gamma(t), \hat{c}^{\dagger}_{\gamma'}(t')\right\}\rangle \\ &= \delta(t-t')\langle\left\{\hat{c}_\gamma(t), \hat{c}^{\dagger}_{\gamma'}(t')\right\}\rangle - i\theta(t-t')\langle\left\{\left[H_0, \hat{c}_\gamma(t)\right], \hat{c}^{\dagger}_{\gamma'}(t')\right\}\rangle \\ &= \delta(t-t')\delta_{\gamma\gamma'} - i\epsilon_\gamma\theta(t-t')\langle\left\{\hat{c}_\gamma(t), \hat{c}^{\dagger}_{\gamma'}(t')\right\}\rangle \\ &= \delta(t-t')\delta_{\gamma\gamma'} + \epsilon_\gamma g^{+}_{\gamma\gamma'}(t,t'). \end{aligned} \tag{39}$$

Here we have used $\partial_t\theta(t) = \delta(t)$ and for the uncoupled system $[H_0, \hat{c}_\gamma] = [\epsilon_\gamma\hat{c}^{\dagger}_\gamma\hat{c}_\gamma, \hat{c}_\gamma] = \epsilon_\gamma\hat{c}_\gamma$. The gammas can refer to any energy level in the system, $\gamma \in \{L, R, Lk_1, Rk_1, Lk_2, Rk_2 \dots\}$. Fourier transforming both sides of the above equation and solving for the Green's function

yields

$$g^+_{\gamma\gamma'}(\omega) = \frac{\delta_{\gamma\gamma'}}{\omega - \epsilon_\gamma + i\eta}. \tag{40}$$

The η is a positive infinitesimal which ensures that the function vanishes for $t < t'$ in accordance with the boundary conditions mentioned in Section 2.4. The Kronecker delta means that $g^+_{\gamma\gamma'}$ is nonzero only for $\gamma = \gamma'$, which is to be expected in the uncoupled case where no correlations are present between the different sites.

Having found the expression for the uncoupled Green's functions, we make use of the Dyson equation [22], which establishes the link between the coupled and uncoupled functions

$$\mathbf{G}^+ = \mathbf{g}^+ + \mathbf{g}^+\mathbf{V}\mathbf{G}^+. \tag{41}$$

Solving the equation for $\mathbf{G}^+$ gives

$$\mathbf{G}^+ = (\mathbb{1} - \mathbf{g}^+\mathbf{V})^{-1}\mathbf{g}^+. \tag{42}$$

The matrix of uncoupled Green's functions is diagonal

$$\mathbf{g}^+ = \begin{pmatrix} g^+_L(\omega) & & & & & & \\ & g^+_R(\omega) & & & & & \\ & & g^+_{Lk_1}(\omega) & & & & \\ & & & g^+_{Rk_1}(\omega) & & & \\ & & & & g^+_{Lk_2}(\omega) & & \\ & & & & & g^+_{Rk_2}(\omega) & \\ & & & & & & \ddots \end{pmatrix} = \begin{pmatrix} \mathbf{g}^+_D & \mathbb{0} \\ \mathbb{0} & \mathbf{g}^+_l \end{pmatrix} \tag{43}$$

and $\mathbf{V}$ is the matrix form of the interaction operator $\hat{V}$

$$\mathbf{V} = \begin{pmatrix} 0 & \Omega & t^*_{Lk_1} & 0 & t_{Lk_2} & 0 & \dots \\ \Omega & 0 & 0 & t^*_{Rk_1} & 0 & t_{Rk_2} & \dots \\ t_{Lk_1} & 0 & 0 & 0 & 0 & 0 & \dots \\ 0 & t_{Rk_1} & 0 & 0 & 0 & 0 & \dots \\ t_{Lk_2} & 0 & 0 & 0 & 0 & 0 & \dots \\ 0 & t_{Rk_2} & 0 & 0 & 0 & 0 & \dots \\ \vdots & \vdots & \vdots & \vdots & \vdots & \vdots & \ddots \end{pmatrix} = \begin{pmatrix} \mathbf{\Omega} & \mathbf{V}^\dagger_l \\ \mathbf{V}_l & \mathbb{0} \end{pmatrix} \tag{44}$$

Here both matrices are also written on block form where the upper left 2x2 block corresponds to inter-dot interactions, the upper right and lower left blocks corresponds to quantum dot-

lead coupling and the lower right block corresponds to lead-lead interaction

$$\mathbf{\Omega} = \begin{pmatrix} 0 & \Omega \\ \Omega & 0 \end{pmatrix}, \qquad \mathbf{V}_l = \begin{pmatrix} t_{Lk_1} & 0 \\ 0 & t_{Rk_1} \\ t_{Lk_2} & 0 \\ 0 & t_{Rk_2} \\ \vdots & \vdots \end{pmatrix}. \tag{45}$$

The same block partition is used for $\mathbf{g}^+$. Using block matrix algebra throughout, we have

$$(\mathbb{1} - \mathbf{g}^+\mathbf{V})^{-1} = \begin{pmatrix} \mathbb{1} - \mathbf{g}_D^+\mathbf{\Omega} & \mathbf{g}_D^+\mathbf{V}_l^\dagger \\ \mathbf{g}_l^+\mathbf{V}_l & \mathbb{1} \end{pmatrix}^{-1}. \tag{46}$$

By the formula for inverse of block matrix (see appendix A.2), the upper-left block of the inverse is given by

$$(\mathbb{1} - \mathbf{g}_D^+\mathbf{\Omega} - \mathbf{g}_D^+\mathbf{V}_l^\dagger\mathbf{g}_l^+\mathbf{V}_l)^{-1} \tag{47}$$

resulting in the retarded Green's function for the quantum dots

$$\begin{aligned} \mathbf{G}_D^+ &= \left[(\mathbb{1} - \mathbf{g}^+\mathbf{V})^{-1}\mathbf{g}^+\right]_D = (\mathbb{1} - \mathbf{g}_D^+\mathbf{\Omega} - \mathbf{g}_D^+\mathbf{V}_l^\dagger\mathbf{g}_l^+\mathbf{V}_l)^{-1}\mathbf{g}_D^+ \\ &= \left[(\mathbf{g}_D^+)^{-1}(\mathbb{1} - \mathbf{g}_D^+\mathbf{\Omega} - \mathbf{g}_D^+\mathbf{V}_l^\dagger\mathbf{g}_l^+\mathbf{V}_l)\right]^{-1} \\ &= \left[(\mathbf{g}_D^+)^{-1} - \mathbf{\Omega} - \mathbf{V}_l^\dagger\mathbf{g}_l^+\mathbf{V}_l\right]^{-1}. \end{aligned} \tag{48}$$

Here one can identify $(\mathbf{g}_D^+)^{-1} - \mathbf{\Omega} = \omega\mathbb{1} - [\mathbf{H}_0]_D - \mathbf{\Omega} = \omega\mathbb{1} - \mathbf{H}_D$ and define the self energy

$$\mathbf{V}_l^\dagger\mathbf{g}_l^+\mathbf{V}_l = \begin{pmatrix} \sum_k \frac{|t_{Lk}|^2}{\omega - \epsilon_{Lk} + i\eta} & 0 \\ 0 & \sum_k \frac{|t_{Rk}|^2}{\omega - \epsilon_{Rk} + i\eta} \end{pmatrix} = \begin{pmatrix} \Sigma_L & 0 \\ 0 & \Sigma_R \end{pmatrix} \equiv \mathbf{\Sigma}^+. \tag{49}$$

This yields the final matrix form for the retarded Green's functions

$$\mathbf{G}_D^+ = (\omega\mathbb{1} - \mathbf{H}_D - \mathbf{\Sigma}^+)^{-1}. \tag{50}$$

For later convenience (e.g. to be able to assume the wide-band limit), we define the energy shift $\mathbf{\Lambda}$ and level width $\mathbf{\Gamma}$ as the real part and minus half the imaginary part of the self-energy,

respectively[1]

$$\mathbf{\Lambda} = \operatorname{Re}\mathbf{\Sigma}^{+} = \begin{pmatrix} \sum_k \mathcal{P}\left\{\frac{|t_{Lk}|^2}{\omega-\epsilon_{Lk}}\right\} & 0 \\ 0 & \sum_k \mathcal{P}\left\{\frac{|t_{Rk}|^2}{\omega-\epsilon_{Rk}}\right\} \end{pmatrix} \tag{51}$$

$$\mathbf{\Gamma} = -2\operatorname{Im}\mathbf{\Sigma}^{+} = \begin{pmatrix} 2\pi\sum_k |t_{Lk}|^2\delta(\omega-\epsilon_{Lk}) & 0 \\ 0 & 2\pi\sum_k |t_{Rk}|^2\delta(\omega-\epsilon_{Rk}) \end{pmatrix}. \tag{52}$$

such that $\Sigma_\alpha = \Lambda_\alpha - \frac{i}{2}\Gamma_\alpha$.

4.2 Lesser Green's functions

Following the result of [23], the lesser self-energy is given by the diagonal matrix

$$\mathbf{\Sigma}^{<} = i\mathbf{\Gamma}\mathbf{f} \tag{53}$$

where $\mathbf{\Gamma}$ is the line width from the previous section and $\mathbf{f}$ is the matrix of Fermi-Dirac distributions for the left and right leads

$$\mathbf{f} = \begin{pmatrix} f_L(\omega) & 0 \\ 0 & f_R(\omega) \end{pmatrix} = \begin{pmatrix} \frac{1}{\exp(\beta_L(\omega-\mu_L))+1} & 0 \\ 0 & \frac{1}{\exp(\beta_R(\omega-\mu_R))+1} \end{pmatrix}. \tag{54}$$

The inverse temperature in the exponent is $\beta_i = 1/k_B T_i$. If not otherwise stated, we will assume equal chemical potential $\mu_L = \mu_R = 0$. Given this self-energy and the retarded/advanced Green's functions (50) and (30), the matrix of lesser Green's functions for the central region can be calculated from the relation [23]

$$\mathbf{G}_D^{<} = \mathbf{G}_D^{+}\mathbf{\Sigma}^{<}\mathbf{G}_D^{-}. \tag{55}$$

4.3 Density operator

The concurrence (35) is calculated from the density matrix ρ of the quantum dot system $\mathcal{S}_D$. We therefore set out to find a general expression connection the Green's functions of the earlier sections to the elements of the density matrix. Expanding $\hat{\rho}$ in the occupation number basis yields

$$\hat{\rho} = \sum_{n_L,n_R,n'_L,n'_R} |n_L, n_R\rangle \langle n'_L, n'_R| \, C^{n_L n_R}_{n'_L n'_R} \tag{56}$$

[1]Here $\mathcal{P}$ denotes the Cauchy principal value of complex analysis.

where we can use (10) to write the coefficients C as

$$C^{n_L n_R}_{n'_L n'_R} = \langle n_L n_R| \hat{\rho} |n'_L n'_R\rangle = \mathrm{Tr}\left\{\hat{\rho}(\hat{c}^\dagger_L)^{n'_L}(\hat{c}^\dagger_R)^{n'_R} |0,0\rangle \langle 0,0| \hat{c}^{n_R}_R \hat{c}^{n_L}_L\right\}. \tag{57}$$

Now we make use of the fact that the projection operator onto the vacuum state can be expressed in terms of creation and annihilation operators as $|0,0\rangle\langle 0,0| = (\mathbb{1}-\hat{c}^\dagger_L\hat{c}_L)(\mathbb{1}-\hat{c}^\dagger_R\hat{c}_R)$. This allows us to write the correlation functions as sums of expectation values of second quantization operators. Expectation values of four operators can be rewritten in terms of simple two-operator expectations by the use of a corollary to Wick's theorem [24]

$$\langle \hat{c}^\dagger_i \hat{c}^\dagger_j \hat{c}_k \hat{c}_l\rangle = \langle \hat{c}^\dagger_i \hat{c}_l\rangle\langle \hat{c}^\dagger_j \hat{c}_k\rangle - \langle \hat{c}^\dagger_i \hat{c}_k\rangle\langle \hat{c}^\dagger_j \hat{c}_l\rangle. \tag{58}$$

Using the fact that expectation values of an uneven number of creation and annihilation operators vanish, we get that the nonzero components of the density matrix are given by

$$\begin{aligned}
C^{11}_{11} &= \langle \hat{c}^\dagger_L \hat{c}_L\rangle\langle \hat{c}^\dagger_R \hat{c}_R\rangle - \langle \hat{c}^\dagger_L \hat{c}_R\rangle\langle \hat{c}^\dagger_R \hat{c}_L\rangle \\
C^{00}_{00} &= \left(1 - \langle \hat{c}^\dagger_L \hat{c}_L\rangle\right)\left(1 - \langle \hat{c}^\dagger_R \hat{c}_R\rangle\right) - \langle \hat{c}^\dagger_L \hat{c}_R\rangle\langle \hat{c}^\dagger_R \hat{c}_L\rangle \\
C^{10}_{10} &= \langle \hat{c}^\dagger_L \hat{c}_L\rangle\left(1 - \langle \hat{c}^\dagger_R \hat{c}_R\rangle\right) + \langle \hat{c}^\dagger_L \hat{c}_R\rangle\langle \hat{c}^\dagger_R \hat{c}_L\rangle \\
C^{01}_{01} &= \langle \hat{c}^\dagger_R \hat{c}_R\rangle\left(1 - \langle \hat{c}^\dagger_L \hat{c}_L\rangle\right) + \langle \hat{c}^\dagger_L \hat{c}_R\rangle\langle \hat{c}^\dagger_R \hat{c}_L\rangle \\
C^{10}_{01} &= \langle \hat{c}^\dagger_R \hat{c}_L\rangle \\
C^{01}_{10} &= \langle \hat{c}^\dagger_L \hat{c}_R\rangle
\end{aligned} \tag{59}$$

and all other C's vanish. The matrix form of $\hat{\rho}$ is

$$\hat{\rho} = \begin{pmatrix} C^{00}_{00} & 0 & 0 & 0 \\ 0 & C^{10}_{10} & C^{10}_{01} & 0 \\ 0 & C^{01}_{10} & C^{01}_{01} & 0 \\ 0 & 0 & 0 & C^{11}_{11} \end{pmatrix}. \tag{60}$$

Up to a factor i, the two-operator expectation values in (59) are exactly the lesser Green's functions (28) evaluated at $t = t'$, which were calculated in Section 4.2.

5 Results

5.1 Explicit expressions of the Green's functions

The retarded Green's functions in the frequency domain are given by the four elements of inverse expression (50)

$$G^+_{LL}(\omega) = \frac{\omega - \epsilon_R - \Lambda_R(\omega) + \frac{i}{2}\Gamma_R(\omega)}{\left[\omega - \epsilon_L - \Lambda_L(\omega) + \frac{i}{2}\Gamma_L(\omega)\right]\left[\omega - \epsilon_R - \Lambda_R(\omega) + \frac{i}{2}\Gamma_R(\omega)\right] - \Omega^2} \tag{61}$$

$$G^+_{RR}(\omega) = \frac{\omega - \epsilon_L - \Lambda_L(\omega) + \frac{i}{2}\Gamma_L(\omega)}{\left[\omega - \epsilon_L - \Lambda_L(\omega) + \frac{i}{2}\Gamma_L(\omega)\right]\left[\omega - \epsilon_R - \Lambda_R(\omega) + \frac{i}{2}\Gamma_R(\omega)\right] - \Omega^2} \tag{62}$$

$$G^+_{LR}(\omega) = G^+_{RL}(\omega) = \frac{\Omega}{\left[\omega - \epsilon_L - \Lambda_L(\omega) + \frac{i}{2}\Gamma_L(\omega)\right]\left[\omega - \epsilon_R - \Lambda_R(\omega) + \frac{i}{2}\Gamma_R(\omega)\right] - \Omega^2}. \tag{63}$$

To express the Lesser Green's functions, we first apply the wide-band limit by absorbing Λ into ϵ and assuming that the level widths are independent of frequency

$$\Lambda(\omega) + \epsilon \to \epsilon, \qquad \Gamma(\omega) \to \Gamma. \tag{64}$$

The wide-band limit is accurate if the density of states of the fermions is constant near the Fermi energy [25]. The formula (55) now yields the four elements of $\mathbf{G}^<_D$

$$G^<_{LL}(\omega) = i\frac{f_L\Gamma_L\left|\omega - \epsilon_R + \frac{i}{2}\Gamma_R\right|^2 + \Omega^2 f_R\Gamma_R}{\left|(\omega - \epsilon_L + \frac{i}{2}\Gamma_L)(\omega - \epsilon_R + \frac{i}{2}\Gamma_R) - \Omega^2\right|^2} \tag{65}$$

$$G^<_{RR}(\omega) = i\frac{f_R\Gamma_R\left|\omega - \epsilon_L + \frac{i}{2}\Gamma_L\right|^2 + \Omega^2 f_L\Gamma_L}{\left|(\omega - \epsilon_L + \frac{i}{2}\Gamma_L)(\omega - \epsilon_R + \frac{i}{2}\Gamma_R) - \Omega^2\right|^2} \tag{66}$$

$$G^<_{LR}(\omega) = i\Omega\frac{(\omega - \epsilon_R + \frac{i}{2}\Gamma_R)f_L\Gamma_L + (\omega - \epsilon_L - \frac{i}{2}\Gamma_L)f_R\Gamma_R}{\left|(\omega - \epsilon_L + \frac{i}{2}\Gamma_L)(\omega - \epsilon_R + \frac{i}{2}\Gamma_R) - \Omega^2\right|^2} \tag{67}$$

$$G^<_{RL}(\omega) = i\Omega\frac{(\omega - \epsilon_L + \frac{i}{2}\Gamma_L)f_R\Gamma_R + (\omega - \epsilon_R - \frac{i}{2}\Gamma_R)f_L\Gamma_L}{\left|(\omega - \epsilon_L + \frac{i}{2}\Gamma_L)(\omega - \epsilon_R + \frac{i}{2}\Gamma_R) - \Omega^2\right|^2}. \tag{68}$$

These are the lesser Green's functions that we seek, but given in the frequency domain. The last step is now to evaluate the Fourier transform from frequency to time

$$G^<_{LL}(\tau) = \mathcal{F}^{-1}[G^<_{LL}(\omega)] = \frac{i}{2\pi}\int_{-\infty}^{\infty}\frac{f_L\Gamma_L\left|\omega - \epsilon_R + \frac{i}{2}\Gamma_R\right|^2 + \Omega^2 f_R\Gamma_R}{\left|(\omega - \epsilon_L + \frac{i}{2}\Gamma_L)(\omega - \epsilon_R + \frac{i}{2}\Gamma_R) - \Omega^2\right|^2}e^{-i\omega\tau}\mathrm{d}\omega \tag{69}$$

and similar integrals for $G^<_{RR}, G^<_{LR}$ and $G^<_{RL}$. The dependence of the transformed function is the time difference $t - t' = \tau$. Analytic solutions to limiting cases of these Fourier integrals

are presented in the following section.

5.2 Limiting cases

5.2.1 Vanishing inter-dot coupling

It is clear that in the limit $\Omega \to 0$, (65), (66), (67), (68) reduce to

$$G^<_{LL}(\omega) = i\frac{f_L\Gamma_L}{\left|\omega - \epsilon_L + \frac{i}{2}\Gamma_L\right|^2}, \quad G^<_{RR}(\omega) = i\frac{f_R\Gamma_R}{\left|\omega - \epsilon_R + \frac{i}{2}\Gamma_R\right|^2}, \quad G^<_{LR}(\omega) = G^<_{LR}(\omega) = 0 \quad (70)$$

The vanishing off-diagonal Green's is reasonable in this limit, since $\Omega \to 0$ leaves the left and right system as two separate systems with no coupling between them. Without explicitly solving the integrals for $G^<(\tau)$, it can be shown that the concurrence (35) of the system vanish when the off-diagonal terms vanish. Using the elements of $\hat{\rho}$ given in (59), we find when $\langle \hat{c}^\dagger_R \hat{c}_L\rangle = \langle \hat{c}^\dagger_L \hat{c}_R\rangle = 0$:

$$\hat{\rho}\tilde{\rho} = \langle \hat{c}^\dagger_L \hat{c}_L\rangle\langle \hat{c}^\dagger_R \hat{c}_R\rangle \left(1 - \langle \hat{c}^\dagger_L \hat{c}_L\rangle\right)\left(1 - \langle \hat{c}^\dagger_R \hat{c}_R\rangle\right) \begin{pmatrix} 1 & 0 & 0 & 0 \\ 0 & 1 & 0 & 0 \\ 0 & 0 & 1 & 0 \\ 0 & 0 & 0 & 1 \end{pmatrix} \quad (71)$$

which has four identical eigenvalues $\lambda_1 = \lambda_2 = \lambda_3 = \lambda_4 = \langle \hat{c}^\dagger_L \hat{c}_L\rangle\langle \hat{c}^\dagger_R \hat{c}_R\rangle \left(1 - \langle \hat{c}^\dagger_L \hat{c}_L\rangle\right)\left(1 - \langle \hat{c}^\dagger_R \hat{c}_R\rangle\right)$. This implies that the concurrence $\mathcal{C}\{\hat{\rho}\} = \max\{0, \sqrt{\lambda_1} - \sqrt{\lambda_2} - \sqrt{\lambda_3} - \sqrt{\lambda_4}\} = 0$. We can solve the Fourier integrals if we assume constant Fermi distributions. We therefore set $f_\alpha(\omega) = f_\alpha(\epsilon_\alpha)$, where $\omega = \epsilon_\alpha$ is the peak of $G^<_{\alpha\alpha}(\omega)$. The integrand of the Fourier integral

$$G^<_{\alpha\alpha}(\tau) = \frac{if_\alpha(\epsilon_\alpha)\Gamma_\alpha}{2\pi}\int_{-\infty}^{\infty} \frac{e^{-i\omega\tau}d\omega}{(\omega - \epsilon_\alpha - \frac{i}{2}\Gamma_\alpha)(\omega - \epsilon_\alpha + \frac{i}{2}\Gamma_\alpha)} \quad (72)$$

now has a single pole $\omega = \epsilon_\alpha - \frac{i}{2}\Gamma_\alpha$ in the lower half-plane, with residue

$$\mathrm{Res}_{\omega=\epsilon_\alpha - \frac{i}{2}\Gamma_\alpha}\left\{\frac{e^{-i\omega\tau}}{(\omega - \epsilon_\alpha - \frac{i}{2}\Gamma_\alpha)(\omega - \epsilon_\alpha + \frac{i}{2}\Gamma_\alpha)}\right\} = i\frac{e^{-(\Gamma_\alpha/2 + i\epsilon_\alpha)\tau}}{\Gamma_\alpha}. \quad (73)$$

Applying Jordan's lemma and Cauchy's residue theorem to a semicircle of radius $R \to \infty$ in the lower half plane yields the solution to the integral

$$G^<_{\alpha\alpha}(\tau) = -\frac{if_\alpha(\epsilon_\alpha)\Gamma_\alpha}{2\pi} \cdot 2\pi i \cdot \mathrm{Res} = if_\alpha(\epsilon_\alpha)e^{-(\Gamma_\alpha/2 + i\epsilon_\alpha)\tau} \quad (74)$$

At $\tau = t - t' = 0$, the density matrix is

$$\hat{\rho} = \begin{pmatrix} [1 - f_L(\epsilon_L)]\,[1 - f_R(\epsilon_R)] & 0 & 0 & 0 \\ 0 & f_L(\epsilon_L)\,[1 - f_R(\epsilon_R)] & 0 & 0 \\ 0 & 0 & f_R(\epsilon_R)\,[1 - f_L(\epsilon_L)] & 0 \\ 0 & 0 & 0 & f_L(\epsilon_L) f_R(\epsilon_R) \end{pmatrix} \tag{75}$$

which was shown earlier to result in vanishing concurrence. In fact, the state (75) is a product state

$$\hat{\rho} = \hat{\rho}_R \otimes \hat{\rho}_L = \begin{pmatrix} 1 - f_R(\epsilon_R) & 0 \\ 0 & f_R(\epsilon_R) \end{pmatrix} \otimes \begin{pmatrix} 1 - f_L(\epsilon_L) & 0 \\ 0 & f_L(\epsilon_L) \end{pmatrix} \tag{76}$$

which is expected from two completely separate subsystems.

5.2.2 Symmetric system

In the case of a symmetric system $\epsilon_L = \epsilon_R \equiv \epsilon$ and $\Gamma_L = \Gamma_R \equiv \Gamma$, the Green's functions reduces slightly. For the first diagonal and off-diagonal elements, we get

$$G^<_{LL}(\omega) = i\Gamma \frac{f_L(\omega)\left[(\omega - \epsilon)^2 + \left(\frac{\Gamma}{2}\right)^2\right] + f_R(\omega)\Omega^2}{\left[(\omega - \epsilon - \Omega)^2 + \left(\frac{\Gamma}{2}\right)^2\right]\left[(\omega - \epsilon + \Omega)^2 + \left(\frac{\Gamma}{2}\right)^2\right]} \tag{77}$$

$$G^<_{LR}(\omega) = i\Omega \frac{\Gamma(\omega - \epsilon)\,[f_L(\omega) + f_R(\omega)] + \frac{i}{2}\Gamma^2\,[f_R(\omega) - f_L(\omega)]}{\left[(\omega - \epsilon - \Omega)^2 + \left(\frac{\Gamma}{2}\right)^2\right]\left[(\omega - \epsilon + \Omega)^2 + \left(\frac{\Gamma}{2}\right)^2\right]} \tag{78}$$

and the remaining two elements can be found by interchanging L and R. To be able to easily evaluate the Fourier integral of this function, we again approximate the Fermi distributions as constants $f_\alpha(\omega) = f_\alpha(\epsilon)$:

$$G^<_{LL}(\omega) \approx i\Gamma \frac{f_L(\epsilon)\left[(\omega - \epsilon)^2 + \left(\frac{\Gamma}{2}\right)^2\right] + f_R(\epsilon)\Omega^2}{\left[(\omega - \epsilon - \Omega)^2 + \left(\frac{\Gamma}{2}\right)^2\right]\left[(\omega - \epsilon + \Omega)^2 + \left(\frac{\Gamma}{2}\right)^2\right]} \tag{79}$$

$$G^<_{LR}(\epsilon) \approx i\Omega \frac{\Gamma(\omega - \epsilon)\,[f_L(\epsilon) + f_R(\epsilon)] + \frac{i}{2}\Gamma^2\,[f_R(\epsilon) - f_L(\epsilon)]}{\left[(\omega - \epsilon - \Omega)^2 + \left(\frac{\Gamma}{2}\right)^2\right]\left[(\omega - \epsilon + \Omega)^2 + \left(\frac{\Gamma}{2}\right)^2\right]} \tag{80}$$

The Fourier integrals are evaluated by calculus of residues, yielding at time difference $\tau = t - t' = 0$

$$\begin{aligned} G^<_{LL}(\tau = 0) &\approx i\frac{2\left[f_L(\epsilon) + f_R(\epsilon)\right]\Omega^2 + \Gamma^2 f_L(\epsilon)}{4\Omega^2 + \Gamma^2} \\ G^<_{LR}(\tau = 0) &\approx \Omega\Gamma\frac{f_R(\epsilon) - f_L(\epsilon)}{4\Omega^2 + \Gamma^2}. \end{aligned} \tag{81}$$

Note that this reduces to the uncoupled result (74) in the limit $\Omega \to 0$, as expected. The six nonzero elements of the density matrix are

$$\langle 00|\hat{\rho}|00\rangle = \frac{\Gamma^2[1 - f_L(\epsilon)][1 - f_R(\epsilon)] + 4\Omega^2\left[1 - \frac{f_L(\epsilon)+f_R(\epsilon)}{2}\right]^2}{4\Omega^2 + \Gamma^2} \tag{82}$$

$$\langle 10|\hat{\rho}|10\rangle = \frac{\Gamma^2 f_L(\epsilon)[1 - f_R(\epsilon)] + 4\Omega^2\left[\frac{f_L(\epsilon)+f_R(\epsilon)}{2}\right]\left[1 - \frac{f_L(\epsilon)+f_R(\epsilon)}{2}\right]}{4\Omega^2 + \Gamma^2} \tag{83}$$

$$\langle 01|\hat{\rho}|01\rangle = \frac{\Gamma^2 f_R(\epsilon)[1 - f_L(\epsilon)] + 4\Omega^2\left[\frac{f_L(\epsilon)+f_R(\epsilon)}{2}\right]\left[1 - \frac{f_L(\epsilon)+f_R(\epsilon)}{2}\right]}{4\Omega^2 + \Gamma^2} \tag{84}$$

$$\langle 11|\hat{\rho}|11\rangle = \frac{\Gamma^2 f_L(\epsilon) f_R(\epsilon) + 4\Omega^2\left[\frac{f_L(\epsilon)+f_R(\epsilon)}{2}\right]^2}{4\Omega^2 + \Gamma^2} \tag{85}$$

$$\langle 10|\,\hat{\rho}\,|01\rangle = i\Omega\Gamma\frac{f_R(\epsilon) - f_L(\epsilon)}{4\Omega^2 + \Gamma^2} \tag{86}$$

$$\langle 01|\,\hat{\rho}\,|10\rangle = i\Omega\Gamma\frac{f_L(\epsilon) - f_R(\epsilon)}{4\Omega^2 + \Gamma^2} \tag{87}$$

The concurrence can be calculated from the method described in Section 2.5.1, and is equal to

$$\begin{aligned} \mathcal{C}\{\hat{\rho}\} =& \frac{2\Omega\Gamma|f_L - f_R|}{4\Omega^2 + \Gamma^2} \\ &- \frac{2\Gamma^2}{4\Omega^2 + \Gamma^2}\sqrt{\left[(1 - f_L)(1 - f_R) + \frac{4\Omega^2}{\Gamma^2}\left(1 - \frac{f_L + f_R}{2}\right)^2\right]\left[f_L f_R + \frac{4\Omega^2}{\Gamma^2}\left(\frac{f_L + f_R}{2}\right)^2\right]} \end{aligned} \tag{88}$$

or $\mathcal{C}\{\hat{\rho}\} = 0$ if the above expression is negative.

Plots The concurrence (88) is plotted as a function of scaled temperature $k_B T_L/\epsilon$ in Fig. 2. The same concurrence is also plotted for equal temperatures $T_L = T_R$ and instead as a function of the left chemical potential μ_L/ϵ in Fig. 3a. The right chemical potential μ_R is set to zero. In Fig. 3b is a 2-dimensional plot showing the concurrence as a function of the two

Fermi functions f_L and f_R.

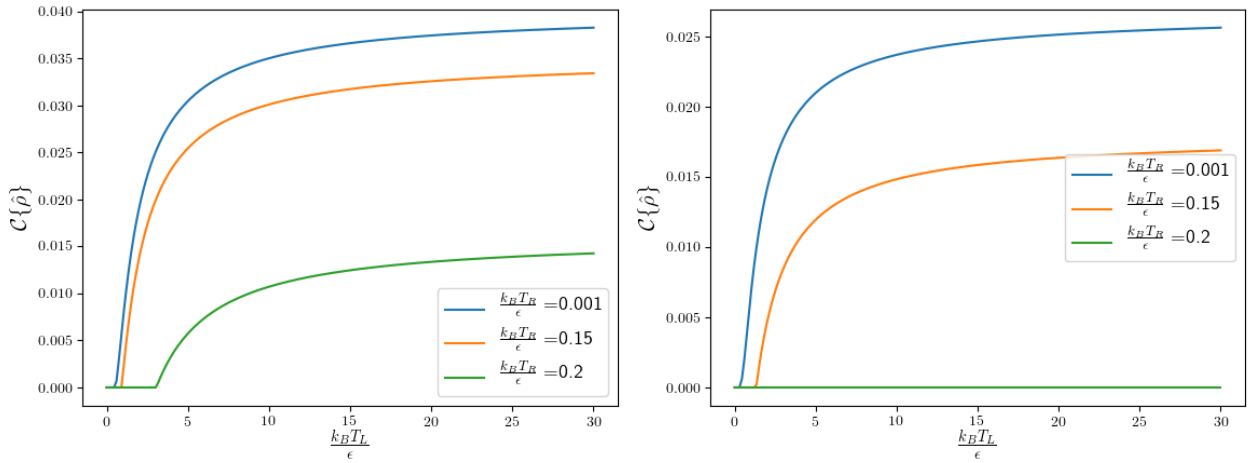

(a) (b)

Figure 2: Concurrence in the symmetric system given by (88). Parameters in (a) are given $\Gamma/\epsilon = 0.01$, $\Omega/\epsilon = 0.002$. Parameters in (b) are given by $\Gamma/\epsilon = 0.01$, $\Omega/\epsilon = 0.001$.

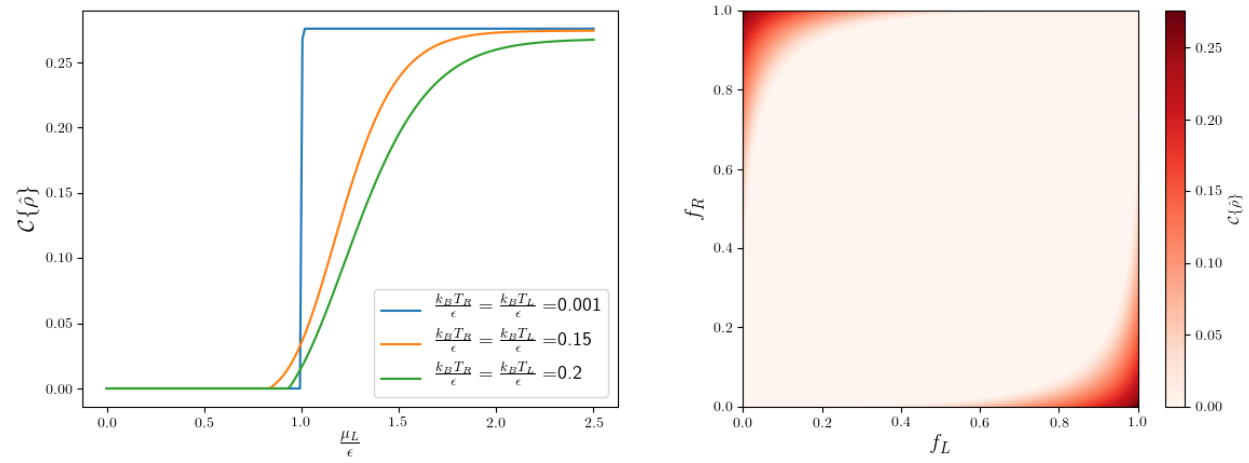

(a) (b)

Figure 3: (a) shows the concurrence plotted as a function of the chemical potential in the left system μ_L/ϵ. The chemical potential in the right system is set to zero $\mu_R = 0$. (b) shows the a 2-dimensional plot of the concurrence as a function of the Fermi functions f_L and f_R. In both cases, parameters are given by $\Gamma/\epsilon = 0.01$, $\Omega/\epsilon = 0.002$.

6 Discussion

6.1 Comments on the results

The concurrence plotted in Fig. 2 can be compared to the result in [2]. We see that our result agrees with the general behaviour of the steady-state concurrence with vanishing Coulomb energy $U/E = 0$, which is presented in Fig. 4c of [2]. This is expected since, as mentioned in Section 3.1, our model does not consider Coulomb interaction in the system.

The concurrence (88) can also be compared to the results from the Markovian master equation approach, see chapter 6 of [26]. There, two qubits in contact with bosonic environments are considered instead of the fermionic system considered here. Interactions are also taken into account here. Comparing the steady state solution $\hat{\rho}$ and the concurrence between the methods, we can see that they result in similar expressions. However, where the concurrence in the bosonic model is zero above some threshold temperature $T_R > T_{\text{threshold}}$, the fermionic model seems to instead approach some finite limit $0 < \lim_{T_R \to \infty} \mathcal{C}\{\hat{\rho}\} < \infty$. This can be attributed to the minor differences in the models, including the Coloumb interaction which is not present in our model.

It is clear from Fig. 3b that the concurrence is maximized when the difference of the Fermi distributions is large. In Fig. 2 this difference is given by the difference in temperature between the leads. It is also clear that instead of a temperature difference, the concurrence can be driven by a difference in chemical potential, see Fig. 3a. In an experimental setting, applying a difference in chemical potential could correspond to applying a voltage across the system.

6.2 Comments on the approximations used

As mentioned in Section 2.4, the Green's functions are exact solutions to the problem at hand. That is, the retarded Green's functions (61), (62) and (63) are exact solutions to the steady-state system without any interaction between fermions. Further, the lesser Green's functions expressed as a Fourier integrals (69) are exact solutions to the steady-state system in the range of validity of the wide-band limit (i.e. when the tunnel rate between the system and leads is approximately constant), also not considering interactions. It is in principle possible to relax the wide-band limit approximation, but this would require more complicated calculations.

The main approximation used in Section 5.2 to be able to evaluate the solutions analytically is the evaluation of the Fermi distributions at constant energy $f(\omega) \to f(\epsilon)$. This simplifies the calculations since it removes the infinitude of poles in the complex plane that

$G^<(\omega)$ would otherwise exhibit. Reducing the number of poles to four allows for the calculation of the Fourier integral (69) using calculus of residues. Relaxing this approximation would require more advanced techniques to solve the integral analytically. One option of solving this more exactly would also be to evaluate the Fourier integrals numerically. This would allow for results which are more generally accurate than those presented by Markovian master equations.

7 Outlook

As discussed in the previous section, more advanced analytical methods could present several ways to expand on the results in this thesis. Numerical methods could also be introduced to solve the Fourier integrals with relaxed assumption. Using a combination of Green's functions and numerical methods should give accurate results outside the range of validity of Markovian master equations. These results would then extent the results of earlier research [2] limited by the approximations implicit in the master equation method [14].

Further, the Green's function method can be extended to include interactions. Calculating the concurrence in this system in a more general setting, as well as further analysing the current results, would allow for more thorough investigation of the impact of the different parameters in the system. For applications the most efficient configuration of parameters are desired, which in this case could be the choice of parameters that maximize the concurrence. The search for this set of parameters could be one goal of further studying this system.

The study of this system with a Green's functions approach is also not limited to concurrence. Any quantity that can be extracted from the density matrix can be calculated by virtually the same process as the one presented in this thesis. Such quantities include heat currents and electrical currents. There is also a possibility to analyze the results of the Green's functions method on this system in relation to thermodynamical uncertainty relations.

Finally, to describe experiments reliably, we need to take into account both interactions and spin. While challenging, this is a promising avenue to pursue. Depending on the implementation, a realistic system would still not be modelled fully by such a simple model. The system in this work is merely a simplified one, and one would hope that implementations are possible where the effects and properties studied here are the major contributions to the behaviour of the system. Nonetheless, results in this simplified domain could be useful for future experimental system design in the nano scales.

A Mathematical tools

A.1 The Fourier Transform

The Fourier transform of a time-dependent function $f(t)$, sometimes denoted by $\mathcal{F}[f]$, is defined as

$$\mathcal{F}[f(t)](\omega) = \int_{-\infty}^{\infty} dt f(t) e^{i\omega t}. \tag{89}$$

Note that the transformed function is not a function of the time variable t, but instead a function of the angular frequency ω. The transformed function is therefore often denoted simply by $f(\omega)$. There also exist an inverse transformation $f(\omega) \to f(t)$ defined by

$$\mathcal{F}^{-1}[f(\omega)](t) = \frac{1}{2\pi} \int_{-\infty}^{\infty} d\omega f(\omega) e^{-i\omega t} = f(t). \tag{90}$$

Properties Useful rules that hold for the Fourier transform includes

$$\mathcal{F}[f] = \mathcal{F}[g] \implies f = g \qquad \text{(uniqueness)} \tag{91}$$

$$\mathcal{F}[c_1 f + c_2 g] = c_1 \mathcal{F}[f] + c_2 \mathcal{F}[g] \qquad \text{(linear)} \tag{92}$$

$$\mathcal{F}[\partial_t f(t)] = -i\omega \mathcal{F}[f] \qquad \text{(transform of the differential operator)} \tag{93}$$

$$\mathcal{F}[\delta(t)] = 1 \qquad \text{(transform of delta function).} \tag{94}$$

Based on the properties above, the Fourier transform proves to be a useful tool to solve certain equations, most notably differential equations. If we want to solve a differential equation in terms of some function $f(t)$, we can transform differential equations to ω-space where the differential operator is mapped to $-i\omega$. In this domain, the problem of solving the differential is mapped to the problem of simply solving the desired function as a function of ω. By uniqueness, one can then evaluate the inverse transform of $f(\omega)$ and arrive at the desired expression for f in the time domain.

A.2 Block matrix algebra

Inversion Assume two block matrices

$$\mathbf{A} = \begin{pmatrix} \mathbf{A}_{11} & \mathbf{A}_{12} \\ \mathbf{A}_{21} & \mathbf{A}_{22} \end{pmatrix}, \qquad \mathbf{B} = \begin{pmatrix} \mathbf{B}_{11} & \mathbf{B}_{12} \\ \mathbf{B}_{21} & \mathbf{B}_{22} \end{pmatrix}. \tag{95}$$

If $\mathbf{AB} = \mathbb{1}$ (i.e. $\mathbf{B} = \mathbf{A}^{-1}$) and assuming $\mathbf{A}_{22}$ is invertible, then

$$\begin{cases} \mathbf{A}_{11}\mathbf{B}_{11} + \mathbf{A}_{12}\mathbf{B}_{21} = \mathbb{1} \\ \mathbf{A}_{21}\mathbf{B}_{11} + \mathbf{A}_{22}\mathbf{B}_{21} = \mathbb{0} \end{cases} . \tag{96}$$

solving this linear system for $\mathbf{B}_{11}$ yields the first sector of $\mathbf{B}$ in terms of $\mathbf{A}$

$$\mathbf{B}_{11} = \left[\mathbf{A}_{11} - \mathbf{A}_{12}\mathbf{A}_{22}^{-1}\mathbf{A}_{21}\right]^{-1} \tag{97}$$

if the inverse on the right-hand side exists.

References

[1] R. Horodecki, P. Horodecki, M. Horodecki, and K. Horodecki, "Quantum entanglement," *Rev. Mod. Phys.*, vol. 81, pp. 865–942, Jun 2009.

[2] J. Bohr Brask, G. Haack, N. Brunner, and M. Huber, "Autonomous quantum thermal machine for generating steady-state entanglement," *New Journal of Physics*, vol. 17, no. 11, p. 9, 2015.

[3] M. T. Mitchison, "Quantum thermal absorption machines: refrigerators, engines and clocks," *Contemporary Physics*, vol. 60, no. 2, pp. 164–187, 2019.

[4] R. Kosloff and A. Levy, "Quantum heat engines and refrigerators: Continuous devices," *Annual Review of Physical Chemistry*, vol. 65, no. 1, pp. 365–393, 2014. PMID: 24689798.

[5] J. P. Pekola, "Towards quantum thermodynamics in electronic circuits," *Nature Physics*, vol. 11, pp. 118–123, Feb 2015.

[6] H. Thierschmann, R. Sánchez, B. Sothmann, H. Buhmann, and L. W. Molenkamp, "Thermoelectrics with coulomb-coupled quantum dots," *Comptes Rendus Physique*, vol. 17, no. 10, pp. 1109 – 1122, 2016. Mesoscopic thermoelectric phenomena / Phénomènes thermoélectriques mésoscopiques.

[7] D. Jacobsson, F. Panciera, J. Tersoff, M. C. Reuter, S. Lehmann, S. Hofmann, K. A. Dick, and F. M. Ross, "Interface dynamics and crystal phase switching in gaas nanowires," *Nature*, vol. 531, pp. 317–322, Mar 2016.

[8] M. Nilsson, F. V. n. Boström, S. Lehmann, K. A. Dick, M. Leijnse, and C. Thelander, "Tuning the two-electron hybridization and spin states in parallel-coupled inas quantum dots," *Phys. Rev. Lett.*, vol. 121, p. 156802, Oct 2018.

[9] M. Josefsson, A. Svilans, A. M. Burke, E. A. Hoffmann, S. Fahlvik, C. Thelander, M. Leijnse, and H. Linke, "A quantum-dot heat engine operating close to the thermodynamic efficiency limits," *Nature Nanotechnology*, vol. 13, pp. 920–924, Oct 2018.

[10] M. P. Woods, R. Silva, and J. Oppenheim, "Autonomous quantum machines and finite-sized clocks," *Annales Henri Poincaré*, vol. 20, pp. 125–218, Jan 2019.

[11] A. Tavakoli, G. Haack, M. Huber, N. Brunner, and J. B. Brask, "Heralded generation of maximal entanglement in any dimension via incoherent coupling to thermal baths," *Quantum*, vol. 2, p. 73, Jun 2018.

[12] Y. Lin, J. P. Gaebler, F. Reiter, T. R. Tan, R. Bowler, A. S. Sørensen, D. Leibfried, and D. J. Wineland, "Dissipative production of a maximally entangled steady state of two quantum bits," *Nature*, vol. 504, pp. 415–418, Dec 2013.

[13] B. Kraus, H. P. Büchler, S. Diehl, A. Kantian, A. Micheli, and P. Zoller, "Preparation of entangled states by quantum markov processes," *Phys. Rev. A*, vol. 78, p. 042307, Oct 2008.

[14] P. P. Hofer, M. Perarnau-Llobet, L. D. M. Miranda, G. Haack, R. Silva, J. B. Brask, and N. Brunner, "Markovian master equations for quantum thermal machines: local versus global approach," *New Journal of Physics*, vol. 19, p. 123037, dec 2017.

[15] A. Tavakoli, G. Haack, N. Brunner, and J. B. Brask, "Autonomous multipartite entanglement engines," *Phys. Rev. A*, vol. 101, p. 012315, Jan 2020.

[16] J. J. Sakurai and J. Napolitano, *Modern Quantum Mechanics*. Cambridge University Press, 2 ed., 2017.

[17] H. Bruus and K. Flensberg, *Many-Body Quantum Theory in Condensed Matter Physics*. Oxford University Press, 2004.

[18] K. Blum, *Density Matrix Theory and Applications*. Springer, Berlin, Heidelberg, 2012.

[19] M. A. Nielsen and I. L. Chuang, *Quantum Computation and Quantum Information: 10th Anniversary Edition*. Cambridge University Press, 2010.

[20] K. F. Riley, M. P. Hobson, and S. J. Bence, *Mathematical Methods for Physics and Engineering: A Comprehensive Guide*. Cambridge University Press, 3 ed., 2006.

[21] G. Mahan, *Many-Particle Physics*. Plenum Press, 1990.

[22] M. M. Odashima, B. G. Prado, and E. Vernek, "Pedagogical introduction to equilibrium green's functions: condensed-matter examples with numerical implementations," *Revista Brasileira de Ensino de Física*, vol. 39, no. 1, 2017.

[23] Y. Meir and N. S. Wingreen, "Landauer formula for the current through an interacting electron region," *Phys. Rev. Lett.*, vol. 68, pp. 2512–2515, Apr 1992.

[24] L. G. Molinari, "Notes on wick's theorem in many-body theory," 2017. arXiv:1710.09248 [math-ph].

[25] C. J. O. Verzijl, J. S. Seldenthuis, and J. M. Thijssen, "Applicability of the wide-band limit in dft-based molecular transport calculations," *The Journal of Chemical Physics*, vol. 138, no. 9, p. 094102, 2013.

[26] P. P. Potts, "Introduction to quantum thermodynamics (lecture notes)," 2019. arXiv:1906.07439 [quant-ph].